8th International Conference on Photonic Technologies LANE 2014

GMA-laser hybrid welding of high-strength fine-grain structural steel with an inductive preheating

Rabi Lahdo[a],*, Oliver Seffer[a], André Springer[a], Stefan Kaierle[a], Ludger Overmeyer[a]

[a]Laser Zentrum Hannover e.V. ,Hannover 30419, Germany

Abstract

The industrial use of GMA-laser hybrid welding has increased in the last 10 years, due to the brilliant quality of the laser beam radiation, and higher laser output powers. GMA-laser hybrid welding processes operate in a common molten pool. The combination of the laser beam and the arc results in improved welding speed, penetration depth, heat affected zone and gap bridgeability.

Single-layer, GMA-laser hybrid welding processes have been developed for high-strength fine-grain structural steels with a grade of S690QL and a thickness of 15 mm and 20 mm. In addition, the welding process is assisted by an integrated, inductive preheating process to improve the mechanical properties of the welding seam. By using the determined parameters regarding the energy per unit length, and the preheating temperature, welding seams with high quality can be achieved.

Keywords: GMA-laser hybrid welding; high-strength fine-grain structural steel; inductive preheating

---

Nomenclature

E	energy per unit length
E_{GMA}	energy per unit length of GMA
E_{laser}	energy per unit length of laser
$F_{2/3}$	two- or three-dimensional heat flow
P_{GMA}	deposition rate

* Corresponding author. Tel.: +49-511-2788-358 ; fax: +49-511-2788-100 .
   E-mail address: r.lahdo@lzh.de

$P_{ind.}$	inductive power
Q	heat input
t	plate thickness
$t_{8/5}$	cooling period
T_0	preheating temperature
Wm	weld seam width in middle
Wr	weld seam width at the root
Wt	weld seam width on the top

1. Introduction and motivation

The developments of high-strength water quenched fine-grained structural steels began in the 1960's and 1970's, to limit dead load and to reduce consumption of material (Hubo and Schroeter, 2001). By using these materials, dead load can be reduced due to characterized high yield strength and simultaneously good toughness. Thus, the advantages regarding the mechanical properties in combination with good welding suitability make these steels attractive for applications like offshore constructions (Bruns et al., 2012), mobile cranes, bridges, heavy steel constructions, utility vehicles, and pressure pipelines for hydropower plants (Hubo and Schroeter, 2001). Conventionally, for these applications arc welding methods are used, usually in multi-layer processes with a comparatively low welding speed. Thus, a high production time and consumption of additional materials are necessary.

The single-layer GMA-laser hybrid welding process is an efficient alternative to the arc welding method, combining GMA welding and laser beam welding in one common molten zone. Due to synergy effects, the advantages of both welding processes occur in the process zone. These provide a high welding speed or penetration depth, lower heat input, lower distortion, small heat affected zones and less consumption of additional materials (Lienert et al., 2011). The GMA-laser hybrid welding process can be supported using inductive preheating to influence the welding process and the mechanical properties of the weld seams. It is possible to increase the welding speed by 13% for welding a fine-grain structural steel with a grade of X70 and a thickness of 13 mm (Lahdo et al., 2013).

For the GMA-laser hybrid welding process of water quenched fine-grain structural steel S690QL with a thickness of 15 and 20 mm, it is necessary to use a preheating process to achieve tolerable hardness and brittleness of the weld seam. Especially, the highly focused energy input of the GMA-laser hybrid welding process leads to lower energy per unit length, and thus to a low cooling period $t_{8/5}$ compared to the conventional arc welding processes (Boese, 2008). By using inductive preheating, it is possible to generate a concentrated heat input around the weld seam, and thus, the cooling period $t_{8/5}$ can be increased.

2. General remarks of water quenched fine-grain structural steels

The properties of water quenched fine-grain steels result from the three-stage process route, depending on the chemical composition. In the first step, the steel is hot rolled at the austenitizing temperature to ensure a homogenous microstructure. The following fast cooling down from the austenitizing temperature, leading to a hard martensitic and bainitic structure with a characteristic high load capacity. To reduce the critical hardness and to improve the toughness by relaxing and modifying the structural components, the steel is subsequently annealed (Schroeter, 2003).

In order to weld water quenched steels like S690QL, due to high strength and carbon equivalents, they should be examined in detail. A high carbon equivalent value and low cooling period $t_{8/5}$ lead to cold cracks in both, the weld metal and heat affected zone. There are different useful conceptions to calculate the carbon equivalent (Hubo and Schroeter, 2001):

- CEV = C + Mn/6 + (Cr + Mo + V)/5 + (Cu + Ni)/15
- CET = C + (Mn + Mo)/10 + (Cu + Cr)/20 + Ni/60
- Pcm = C + Si/30 + (Mn + Cu + Cr)/20 + Ni/60 + Mo/15 + V/10 + 5B

Table 1 summarizes the different carbon equivalents and the hardness of the base material for the used materials.

Table 1. Different carbon equivalents and hardness of the base material

Material and plate thickness	CEV [%]	CET [%]	Pcm [%]	Carbon content [%]	Hardness [HV1]
S690QL, t = 15 mm	0.48	0.34	0.29	0.18	270
S690QL, t = 20 mm	0.48	0.33	0.28	0.17	270

The mechanical properties in the weld metal and heat affected zone are characterized by high hardness and low toughness. Fig. 1 shows the resulting hardness in the heat affected zone and toughness depending on the cooling period $t_{8/5}$ of a weld seam of steel S690QL. It has been shown that the cooling period $t_{8/5}$ should be between 10 and 25 second (Hamme et al., 2000). The transition temperature T_{27} describes the temperature which an impact energy of 27 J is achieved.
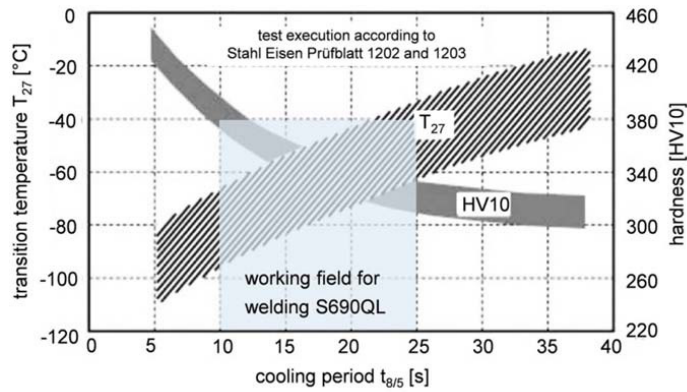

Fig. 1. Hardness and toughness of S690QL depending on the cooling period $t_{8/5}$ (Hamme et al. , 2000).

The cooling period $t_{8/5}$ depends on the welding parameters such as heat input Q, preheating temperature T_0, thickness t and geometry, which can be calculated according to EN1011-2 and SEW 088, see formula (1) and (2). All important factors merge in the cooling period $t_{8/5}$, which behaves proportional to the preheating temperature and the heat input (Hamme et al., 2000). The factors F2 or F3 – two- or three-dimensional heat flow – were chosen depending on the thickness, with a value more or less 18 mm (Kindmann et al., 2012). By increasing the preheating temperature or energy per unit length, the cooling period increases.

$$t_{8/5} = (6700 - 4.3 \cdot T_0) \cdot 10^5 \cdot \frac{Q^2}{t^2}\left[\left(\frac{1}{500 - T_0}\right)^2 - \left(\frac{1}{800 - T_0}\right)^2\right] \cdot F_2 \tag{1}$$

$$t_{8/5} = (6700 - 5 \cdot T_0) \cdot Q \cdot \left(\frac{1}{500 - T_0} - \frac{1}{800 - T_0}\right) \cdot F_3 \tag{2}$$

3. Experimental setup and used materials

The investigations of GMA-laser hybrid welding process were carried out using a solid-state laser with a maximum laser beam power of 6 kW and a welding current source with a maximum current value of 550 A. A filler wire CrNiMo according to DIN EN ISO 14341 was used. As shielding gas an Ar-CO_2 mixed gas with a content of 82 % argon and 18 % CO_2 according to DIN EN ISO 14175 was used. The one-side welding process was developed for a butt joint in a flat position (PA). Before the GMA-laser hybrid welding process is employed, a separate laser welding process bonds the edges. For the preheating process, an induction unit with a maximum power of 40 kW was used. The inductor has an active zone of 40 mm x 30 mm. Fig. 2 shows the real and schematic experimental setup with the GMA-torch, the laser processing head, the workpiece and the inductor.
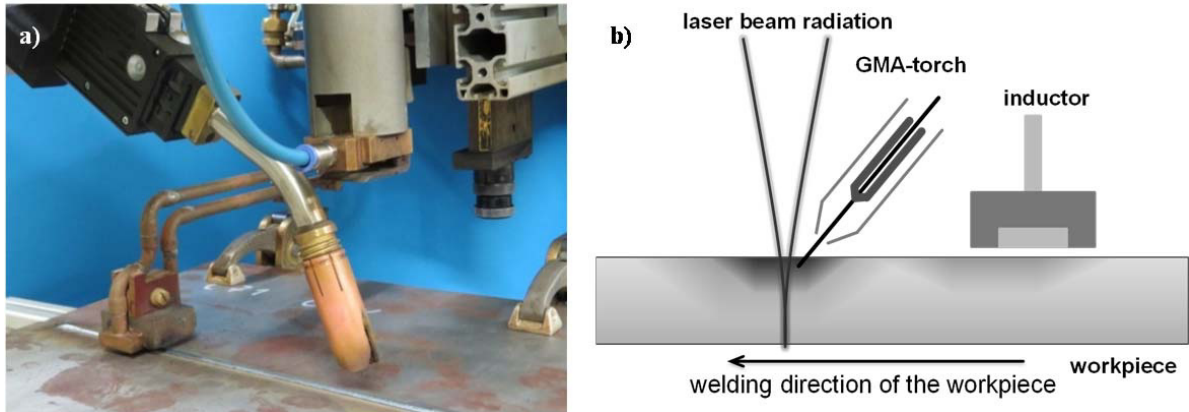

Fig. 2. Real (a) and schematic (b) experimental setup.

The welding parameters for the steel grade S690QL were determined depending on the sheet thickness of 15 mm and 20 mm. For the development of the welding process, the inductive preheating and the energy per unit length are varied to determine the influence on the properties of the weld seam. High quality welding seams were achieved in a single-layer pass with the determined welding parameters. In table 2, the welding parameters are listed.

Table 2. Determined welding parameters.

Material and plate thickness	Welding speed [m/min]	Wire feed rate [m/min]	Edge preparation [-]	Energy per unit length [kJ/m]	Preheating temperature at top / root [°C]
S690QL, t = 15 mm	1.50	10	10°Y8mm	610	140^1 / 120^1; 280^2 / 220^2
	1.00	8	10°Y8mm	800	190^1 / 180^1; 330^2 / 300^2
	0.75	6	10°Y8mm	970	-
S690QL, t = 20 mm	0.75	14	20°Y9mm	1648	300^1 / 250^1; 370^2 / 300^2

by an inductive power $P_{ind.}$ of 20 kW (1) and 40 kW (2)

4. Evaluation procedure: Characterization of the weld seam and hardness

To characterize the weld seam geometry and the metallurgy of the weld seam, cross-sections were taken. By using nital with a concentration of nitric acid of 3%, the microstructure of the weld metal, heat affected zone and base material can be made visible, with precise distinctions to each other. Regarding the geometry of the weld seam, the width on the top (Wt), in middle (Wm) and at the root (Wr) as well as the area of the HAZ are determined. Fig. 3 (a) illustrates schematically the determination of the geometric variables.
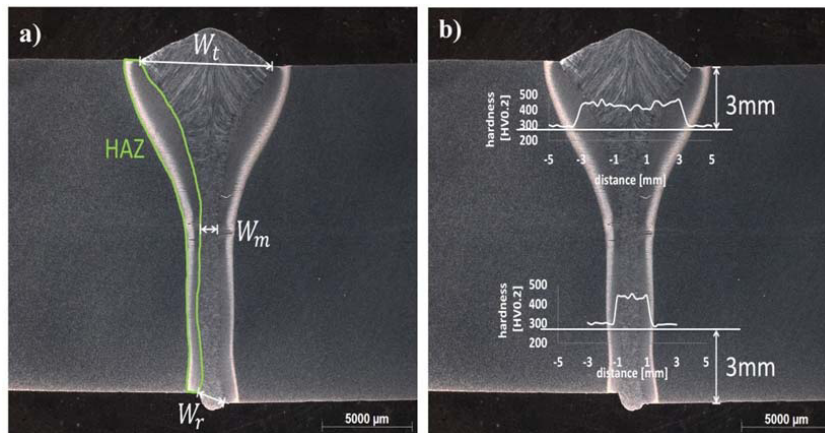

Fig. 3. (a) Determination of the geometric variables; (b) determined hardness profiles.

A hardness test method based on Vickers was done according to DIN EN ISO 6507-1. The hardness profiles of the S690QL were taken at a 3 mm distance from the top/root, see Fig. 3 (b). To test the plates with a thickness of 15 mm, the investigation was performed with a test load of 1.96 N (HV0.2) for exact hardness distribution, due to the possibility of using a narrow distance between hardness indentations of 0.25 mm. For plates with a thickness of 20 mm, tests were carried out with a test load of 98.07 N (HV10) and a distance of 1 mm between the hardness indentations.

5. Results

5.1. Geometry of the weld seam depending on the energy per unit length of S690QL (t =15 mm)

In the context of this investigation, the weld seam geometry was determined in dependency of the energy per unit length. The development of the hybrid welding process was carried out with various energy per unit length values of 610, 800 and 970 kJ/m. Additionally, the energy per unit length was separated in laser and GMA content. Due to a constant laser power of 6 kW and various welding speeds of 0.75, 1.0 and 1.5 m/min, a linear correlation between the welding speed and energy per unit length of the laser results. Fig. 4 shows the results concerning the geometry of the weld seam (a) and the cross-sections of welding seams (b-d), which were joined with varied energy per unit length values.

The cross-sections and the course of the graphs show an increasing width of the root and the middle increasing energy per unit length. Due to a linear increase of energy per unit length of the laser, the weld seam width in the middle (Wm) increases from 0.96 mm to 1.42 mm. Principally, the width on top increases with increasing energy per unit length, but only in combination with increasing deposition rate P_{GMA}. As example, the deposition rate P_{GMA} of c) with a value of 7.4 kW is lower compared to d) with a value of 6.1 kW.
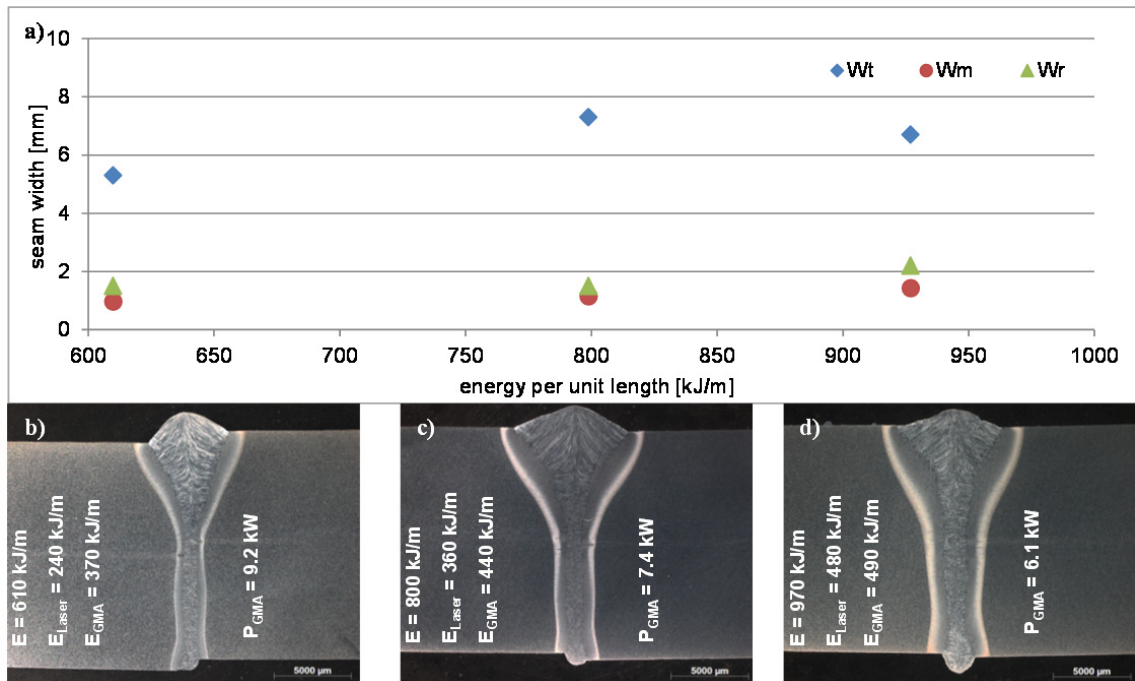
Fig. 4. Influence of the energy per unit length on the geometry of the welding seam, welded with b) 610 kJ/m, c) 800 kJ/m, d) 970 kJ/m.

5.2. Influence of the preheating on the weld seam geometry and hardness of S690QL (t = 15 mm)

For this investigation, two different energy per unit length values for the hybrid welding process and varied inductive power $P_{ind.}$ of 0, 20 and 40 kW were used to influence the weld seam geometry and hardness distribution. All weld seams exhibit a high quality for all investigated configurations regarding the energy per unit length and inductive power. Based on x-ray inspection and cross-sections, no imperfections were observed, except for a few individual pores. The weld reinforcement and root reinforcement are in an acceptable range from 1.5 to 1.7 mm.

The results of the weld seam geometry depending on the inductive power, and an energy per unit length of 610 kJ/m (d) and 800 kJ/m (e) are presented in Fig. 5. In addition, the HAZ are determined in Fig. 5 (c). The width of the weld seam is a result of the welding parameters as shown earlier in Fig. 4. The seam width increases with increasing inductive power depending on the energy per unit length. For the width of the middle and the root of the weld seam, coherence between the weld seam geometry and the inductive power cannot be detected. Based on the cross-sections, the areas of the HAZ were determined. The HAZ increases with increasing inductive power and energy per unit length.

When using water quenched fine-grain structural steel, hardening in the weld metal and the heat affected zone is expected, due to the carbon equivalent. To ensure tough weld joints, the hardness in the weld seam must be reduced. The hardness distribution was investigated for varying inductive power and energy per unit length values. In Fig. 6, the results of the hardness tests are presented. It is possible to reduce the hardness in the weld metal and in the heat affected zone depending on the energy per unit length and inductive power. By using an energy per unit length of 610 kJ/m and an inductive power $P_{ind.}$ of 40 kW, the average hardness is reduced from 430 to 350 HV0.2 in the weld metal at the top. The influence of the inductive assistance regarding the hardness in the heat affected zone cannot be seen, so that the hardness remains constant. Increasing the energy per unit length to 800 kJ/m and simultaneously the inductive preheating, the hardness in the heat affected zone at the top decreases to 385 HV0.2. These welding parameters provide a lower reduction of the hardness in the root compared to the hardness in the top, because of the small molten pool and consequent cooling period. The hardness can be lowered to 410 HV0.2.
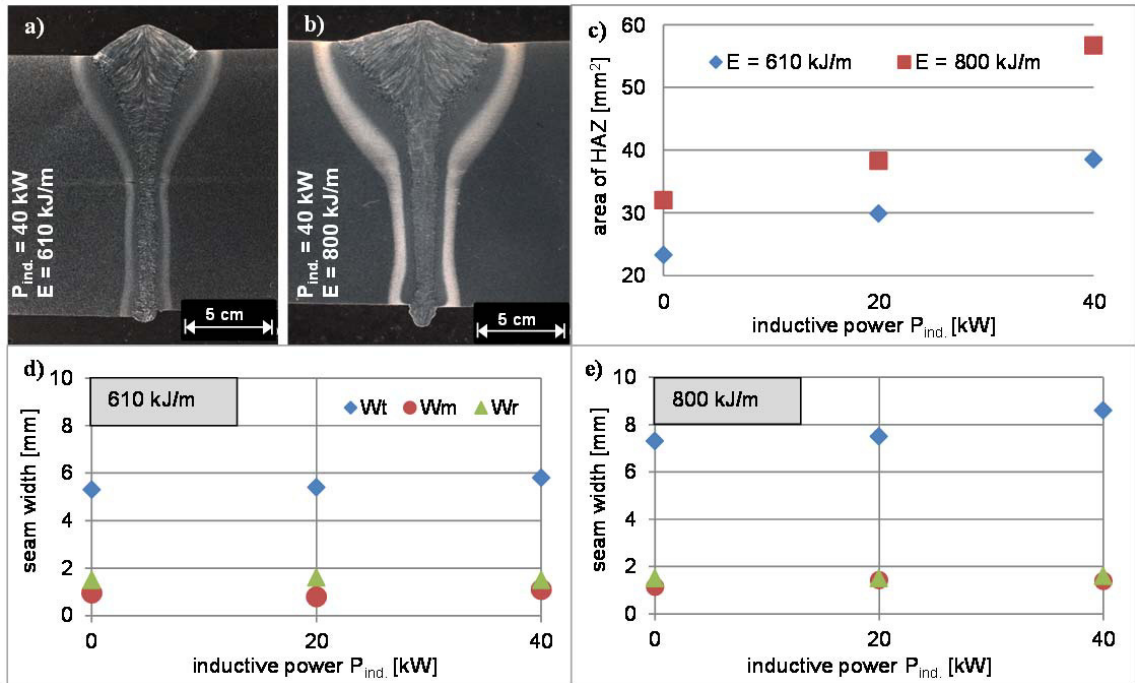
Fig. 5. Cross-sections (a-b) and results of the weld seam geometry and the HAZ (c) depending on the inductive power, and an energy per unit length of 610 kJ/m (d) and 800 kJ/m (e).
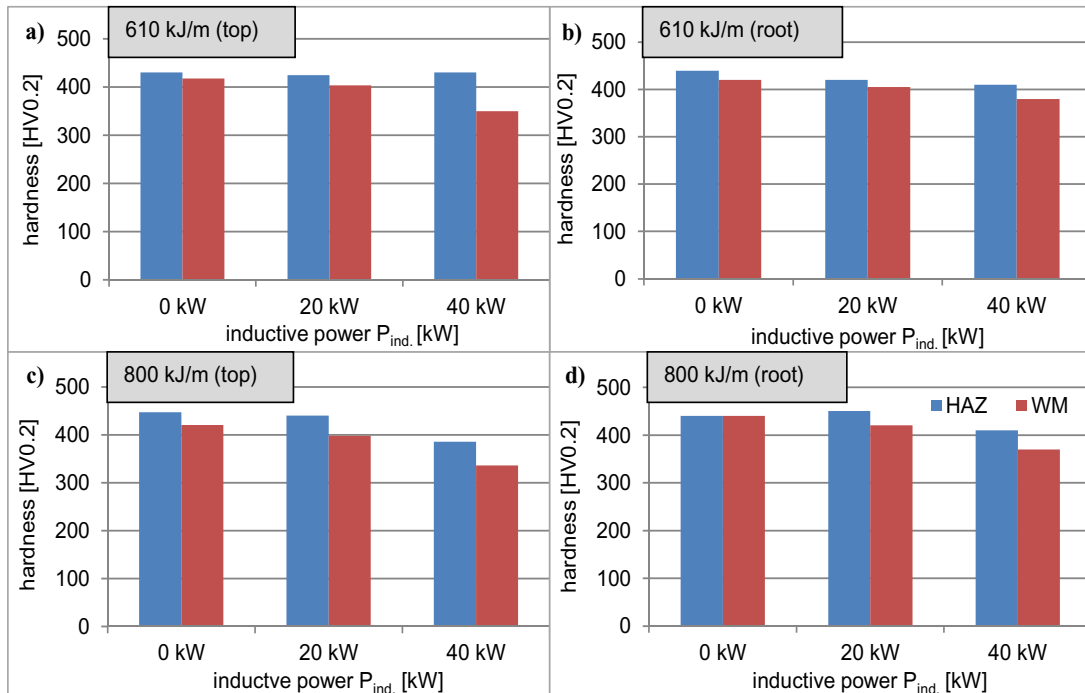

Fig. 6. Hardness of the weld metal and HAZ at the top and the root depending on the energy per unit length and the inductive power, (a) 610 kJ/m at the top, (b) 610 kJ/m at the root, (c) 800 kJ/m at the top and (d) 800 kJ/m at the root.

5.3. Geometry of the welding seam and hardness of S690QL (t = 20 mm)

The GMA-laser hybrid welding process of the steel grade S690QL with a thickness of 20 mm was performed with additional variations of the inductive power, to determine the influence of the inductive power on the weld seam geometry and the hardness. The high quality of the weld seams regarding imperfections was characterized using x-ray inspections and cross-sections. In Fig. 7, cross-sections welded with various inductive powers $P_{ind.}$ of 0, 20 and 40 kW are presented. Based on the cross-sections, it could be determined that the weld seam, especially the width of the seam and the dimension of the HAZ increase with increasing inductive power.
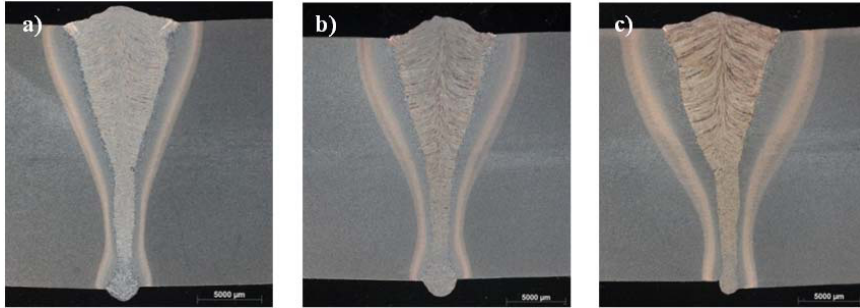

Fig. 7. Cross-sections of welding seam: $P_{ind.}$ = 0 kW (a), 20 kW (b) and 40 kW (c).

The inductive power has an influence on the hardness of steel with the grade of S690QL and a thickness of 20 mm, as could be expected (Fig. 8). The hardness profile on the top and at the root is characterized with hardening in the HAZ, depending on the inductive preheating. Thus, the hardness of the HAZ at the top can be decreased from 410 HV10 without inductive power to 350 HV10 with an inductive power $P_{ind.}$ of 40 kW. In the weld metal, the hardness has a value of 315 HV10 without preheating, and with inductive power $P_{ind.}$ of 40 kW the hardness is reduced to a value of 250 HV10. This hardness level is lower than the hardness of the base material with a value of 270 HV10. The hardness in the HAZ at the root decreases from 410 HV10 to 315 HV10 using an inductive power $P_{ind.}$ of 40 kW.
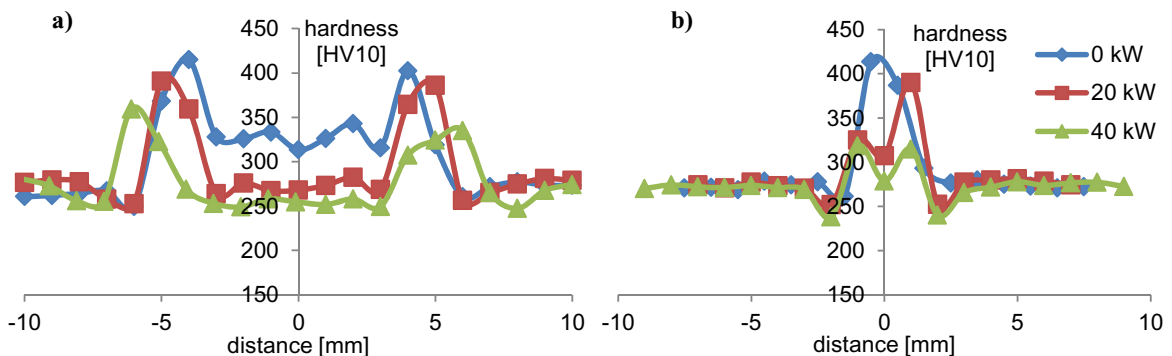

Fig. 8. Hardness distribution at the top (a) and at the root (b) of S690QL with a thickness of 20 mm.

6. Summary and Conclusion

GMA-laser hybrid welding process with supportive inductive preheating is suitable for welding of water quenched fine-grain structural steel grade S690QL with a thickness of 15 and 20 mm. The welding process is performed in one single layer. The weld seams produced are characterized by a high quality and without any imperfections, except for a few individual pores. The influence of the inductive preheating on the weld seam geometry and hardness distribution can be seen. However weld seam geometry regarding the width and the area of the HAZ increase with increasing inductive preheating. The hardness of steel S690QL with a thickness of 15 mm can be reduced to a value near 380 HV0.2 in the upper HAZ and 410 HV0.2 in the lower HAZ by using an energy per unit length of 800 kJ/m and an inductive power $P_{ind.}$ of 40 kW. The hardness of the steel S690QL with a thickness of 20 mm can be decreased from 410 HV10 to 350 HV10.

In addition, the weld seam must be characterized by tensile tests and Charpy impact test, especially to determine the effect of the preheating on the mechanical properties.

Acknowledgements

References

Boese, B., 2008. Laser-MSG-Hybridschweißen von höchstfesten Feinkornbaustählen. Dissertation, Laser Zentrum Hannover e.V..

Bruns, C., Krampen, J., Wiebe, J., 2012. Weldability of High Strength Seamless Pipes for Fixed Offshore Structures. In: Proceedings of the Twenty-second (2012) International Offshore and Polar Engineering Conference, the International Society of Offshore and Polar Engineers, California, pp. 209.

Hamme, U., Hauser, J., Kern, A., Schriever, U., 2000. Einsatz hochfester Baustähle im Mobilkranbau. Stahlbau 69, Heft 4, pp. 295- 305.

Hubo, R., Schroeter, F., 2001. Stähle für den Stahlbau - Auswahl und Anwendung in der Praxis. Stahlbau Kalender 2001, pp. 545-589.

Kindmann, R., Stracke, M., 2012. Verbindungen im Stahl- und Verbundbau. In: Wilhelm Erst & Sohn Verlag, Berlin, pp. 354.

Lahdo, R., Seffer, O., Springer, A., Kaierle, S., Overmeyer, L., Collmann, M., Schaumann, P., Neumeyer, J., Schuelbe, H., Nacke, B., 2013. Induction Assisted GMA-Laser Hybrid Welding of High-Strength Fine-grain Structural Steels, In: Proceedings of the ICALEO Conference, Miami, USA, paper #902.

Lienert, T., Siewert T., Babu, S., Acoff, V., 2011. Hybrid Laser Arc Welding. ASM Handbook, Volume 6A, Welding Fundamentals and Processes, pp. 321.

Schroeter, F., 2003, Höherfeste Stähle für den Stahlbau – Auswahl und Anwendung. Bauingenieur Heft 9, pp. 426-432.